Dynamics of dry friction: A numerical investigation

Y. F. Lim and Kan Chen
Department of Computational Science, National University of Singapore, Singapore 119260
(Received 9 March 1998)

We perform extended numerical simulation of the dynamics of dry friction, based on a model derived from the phenomenological description proposed by Baumberger *et al.* [Nature (London) **367**, 544 (1994)] and Heslot *et al.* [Phys. Rev. E **49**, 4973 (1994)]. Under a quasistationary approximation, the model is related to the Dieterich-Ruina aging (or slowness) law, which was introduced by Dieterich [Pure Appl. Geophys. **116**, 790 (1978); J. Geophys. Res. **84**, 2161 (1979); in *Mechanical Behavior of Crustal Rocks*, edited by N. L. Carter *et al.*, Geophysics Monograph No. 24 (AGU, Washington, DC, 1981), p. 103] and Ruina [J. Geophys. Res. **88**, 10 359 (1983)] on the basis of experiments on rocks. We obtain a dynamical phase diagram that agrees well with the experimental results on the paper-on-paper systems. In particular, the bifurcation between the stick-slip motion and steady sliding is shown to change from a direct (supercritical) Hopf type to an inverted (subcritical) one as the driving velocity increases, in agreement with the experiments.
[S1063-651X(98)01311-7]

PACS number(s): 05.45.+b, 46.30.Pa, 62.20.Hg, 91.30.Px

I. INTRODUCTION

It is well known that frictional resistance is independent of the apparent area of the sliding surface and it is proportional to the normal load with a proportional constant μ, which is known as the friction coefficient. Traditionally, the friction coefficient has two distinct values: the static friction coefficient μ_s, determined from the minimum force needed to move a slider at rest, and the dynamic friction coefficient μ_d, used for the friction force when a steady sliding motion is established. Friction is often described using the well-known Amontons-Coulomb laws: (i) Both μ_s and μ_d are independent of the apparent area of the contacting surfaces and the normal load, (ii) both μ_s and μ_d depend on the shear characteristics of the contacting materials [1,2]; and (iii) for most cases, μ_d is appreciably lower than μ_s. This standard picture is still widely accepted nowadays; however, in many cases, significant refinements must be taken into account for the explanation of the observed friction.

Our common experiences tell us that the sliding of contact bodies subjected to a steady pulling velocity sometimes proceeds in an alternation of periods of rest and sliding rather than moving steadily (this is the reason, for example, for the occurrence of squeaking noises). This unstable motion consists of periods of a stick state followed by a sudden slip and is known as stick-slip oscillations. The stick-slip motion occurs on both large and small scales. Understanding the stick-slip phenomenon is important not only for many engineering applications, but also for understanding the mechanism of earthquakes (which is a stick-slip phenomenon on a geological scale [3]).

Obviously, stick-slip motion is caused by the variation of frictional resistance during sliding. In a certain range of the velocity V, a velocity weakening behavior [corresponding to a decreasing function $\mu_d(V)$ with respect to the steady relative sliding velocity V of the contact surfaces] is often observed in many different materials including metals [2] and rocks [4]. In this range, which generally lies in a low-velocity regime, the steady motion is unstable with respect to perturbation; this gives rise to stick-slip phenomena. On the other hand, the static friction coefficient μ_s is generally found to be an increasing function with respect to the contact age of contact surfaces [4,5]. This can be explained by the fact that the plastic relaxation of the stressed contact junctions during a stick period leads to an increasing real contact area, hence strengthening the contact. The mechanism for the velocity dependence of μ_d and the mechanism for the age dependence of μ_s are not unrelated; both can be understood using the concept of a memory length [6,4].

The purpose of the paper is to show, by explicit numerical simulation, that a model based on the phenomenological description of Ref. [7] can be used to explain qualitatively (and sometimes even quantitatively) many interesting features found in experiments. The model incorporates the existing understanding of the age dependence of the static friction and the velocity dependence of the dynamic friction at low velocity, but does not make a distinction between the dynamic and static frictions. There is no abrupt change from ''static'' friction to ''dynamic'' friction as in the traditional description of friction; this is important for the numerical simulation used to construct the entire phase diagram for the dynamics of dry friction. The rest of the paper is organized as follows. We first review in Sec. II the phenomenology of dry friction, focusing on the work done by Dieterich [6] and Ruina [8] and recent experiments performed by Baumberger and co-workers [9,7]. We then establish in Sec. III the fact that the phenomenological description of Ref. [7] is related to the well-known Dieterich-Ruina aging (or slowness) law [8,10–12] as well as the Ruina-Dieterich slip law. The results from simulation of the model will be presented (Sec. IV) together with some concluding remarks (Sec. V).

II. PHENOMENOLOGY OF DRY FRICTION

Following the pioneering work of Rabinowicz on metals [2], many experimental studies have been performed to study the low-velocity friction properties of various materials. In particular, experiments with rocks suggest a constitutive

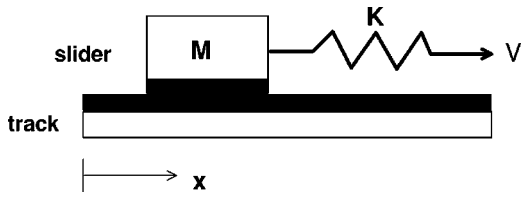

FIG. 1. Schematic block-spring system. The slider with mass M is driven by a pulling velocity V through a spring with stiffness K. The displacement of the center of mass of the slider with respect to the track is x.

framework in which the rock friction can be characterized by a set of evolving state variables. This idea was introduced by Dieterich [6] and was generalized by Ruina [8]. The two frequently used single-state-variable constitutive laws can be described as follows.

(i) The Ruina-Dieterich slip law [10–12]. The friction coefficient μ can be written in terms of the instantaneous velocity v of the slider and the state variable ϕ that characterizes the slip history of the contact:

$$\mu(\phi,v)=\mu_0+A'\ln\frac{v}{v_c}+B'\ln\frac{v_c\phi}{d_c}, \tag{1}$$

$$\dot{\phi}=-\frac{v\phi}{d_c}\ln\frac{v\phi}{d_c}, \tag{2}$$

where μ_0, A', B', v_c, and d_c are constants. This slip law, however, cannot be used to describe restrengthening in stationary contact.

(ii) The Dieterich-Ruina aging (or slowness) law [10–12]. In this law $\mu(\phi,v)$ is given by Eq. (1), but ϕ now satisfies the dynamical equation

$$\dot{\phi}=1-\frac{v\phi}{d_c}. \tag{3}$$

The restrengthening in truly stationary contact is incorporated in this version because $\dot{\phi}=1$ while $v=0$.

In steady sliding motion, both laws give $\phi=d_c/v$ and the steady-state coefficient is $\mu(d_c/v,v)=\mu_0+(A'-B')\ln(v/v_c)$. Moreover, in the case of a small deviation from the steady sliding motion, both laws linearize to the same form [8,13]. Extensive nonlinear stability studies for both one- [Eqs. (1) and (2)] and two-state-variable slip laws have been performed by Gu *et al.* [14].

In a more general constitutive framework the friction coefficient μ can be written in terms of the ''state'' of the contact surfaces, namely, $\mu=\mu(\text{state},v)$ [8]. Ruina and Rice [8,13] consider a general constitutive friction law with $\partial\mu(\text{state},v)/\partial v>0$ and they have established the dynamic linear stability conditions for steady sliding: For a block-spring system as shown in Fig. 1, the steady sliding motion with velocity V is stable when [13]

$$d\mu_{ss}(V)/dV>0 \tag{4}$$

or when

$$d\mu_{ss}(V)/dV<0 \quad \text{with} \quad K>K_{cr},$$

where the critical stiffness is given by

$$K_{cr}=\frac{-MgVd\mu_{ss}(V)/dV}{d_c}\times\left\{1+\frac{V}{d_cg[\partial\mu(\text{state},V)/\partial V]_{\text{state}=\text{state}(V)}}\right\}. \tag{5}$$

In the above expression $\mu_{ss}(V)$ is the steady-state coefficient. We will show that this stability criterion fits our numerical result very well.

On the other hand, an extensive experimental study of the dry friction dynamics of a paper-on-paper block-spring system (shown in Fig. 1) has been performed by Baumberger and co-workers [9,7] recently. Their experiments verified many known properties of dry friction and gave a rather complete picture of dry friction in various regimes. In particular, they explored systematically the dynamical phase diagram by varying the driving velocity V, the slider mass M, and the spring stiffness K. The features of their experiments are summarized as follows.

(i) The phase diagram in control parameter space $(V,K/M)$ consists of two regions that can be characterized by stick-slip motion and steady sliding, respectively, and they are separated by a bifurcation curve. The character of the bifurcation changes from a direct (supercritical) Hopf type in the creep-dominated regime to an inverted (subcritical) one in the inertial regime as V increases.

(ii) In the steady sliding region, the measured dynamic friction coefficient μ_d exhibits velocity weakening in low-velocity range ($\leqslant$0.1 mm/s), which can be fitted as

$$\mu_d(V)|_{lowV}=a_v-b_v\ln(V/V_0), \tag{6}$$

where V_0 is an arbitrary velocity scale, and velocity strengthening at larger velocities, which can be characterized as

$$\mu_d(V)|_{highV}=\mu_d^0+\eta V. \tag{7}$$

(iii) The static friction coefficient μ_s was found to increase with the contact age t_{st} as

$$\mu_s(t_{st})=a_s+b_s\ln(t_{st}). \tag{8}$$

(iv) By introducing a characteristic memory length D_0, a relation between Eqs. (6) and (8), i.e.,

$$\mu_d(V)|_{lowV}=\mu_s(D_0/V), \tag{9}$$

can be established. Here D_0, which is given experimentally as 0.9 μm [7], can be interpreted as an average sliding displacement needed to move to new microcontacts.

These results are rather general (rock-rock friction [6,4], for example, exhibits similar features). The experiments show that the motion of the system at low velocity ($\leqslant$0.1 mm/s) is primarily controlled by a creep process. Based on these results, a phenomenological model of dry friction dynamics for the low-velocity regime [7] of the paper-on-paper system has been proposed. Both linear [7] and nonlinear [15] stability analyses about steady sliding of the model give excellent quantitative agreement with experiments. In addition, the transient behavior in the steady sliding region of the system after setting the driving velocity to zero suddenly has

been studied under the aid of the model [16], where a two-stage process has been observed. However, there is no systematic theoretical study of the entire regime covering the crossover from the static friction regime to the dynamic friction regime and the crossover to the high-velocity (inertial) regime. In this paper we show numerically that most important experimental features in various regimes can be reproduced in a single model.

III. PHENOMENOLOGICAL MODEL

We follow the phenomenological approach used in Ref. [7]. Consider the experimental setup shown in Fig. 1. The motion of the block under the influence of the external driving force as shown in Fig. 1 is assumed to be a thermally activated creeping motion in a periodic pinning potential biased by the external driving force. In the low-bias regime, where the barrier heights of the effective potential are comparable to the thermal activation energy, the velocity of the slider is given by

$$\dot{x}=a\left(\frac{1}{\tau_+}-\frac{1}{\tau_-}\right), \tag{10}$$

where a is the typical distance between two potential minima and τ_+ (τ_-) is the thermal time for escaping from a given well into its downstream (upstream) nearest neighbor. If we let the corresponding barrier height be U_+ (U_-), then we have

$$\frac{1}{\tau_\pm}=\frac{\omega_0}{2\pi}\exp\left\{-\frac{\Delta U_\pm}{\sigma}\right\}, \tag{11}$$

where σ is the thermal activation energy. σ can be written as $N_{cr}RT$, where N_{cr} is the number of moles of the degrees of freedom involved in the creep motion. ω_0 is the oscillation frequency about the minimum of the effective potential. The amplitude ΔU_0 of the periodic pinning potential is assumed to increase with the dynamical contact age variable ϕ [6,8,7], hence the barrier heights are given by

$$\Delta U_\pm=\Delta U_0(\phi)\mp F_{ext}a/2, \tag{12}$$

where F_{ext} is the external force (in the experimental setup, it is the spring force induced by the driving velocity V).

Although Eqs. (10) and (11) are valid strictly only for a time- and position-independent external force and a time-independent pinning potential, they can also be used in more general cases under the assumption that the changes in F_{ext} and $\Delta U_0(\phi)$ are so slow that an *adiabatic* approximation is valid [7]. Combining the above equations we can write the velocity of the slider as

$$\dot{x}(t)\approx\frac{\omega_0 a}{2\pi}2\sinh\left\{\frac{F_{ext}a}{2\sigma}\right\}\exp\left\{-\frac{\Delta U_0}{\sigma}\right\}. \tag{13}$$

In the case that $F_{ext}a\gg\sigma$, the above equation can be approximated as

$$F_{ext}=\frac{2\Delta U_0(\phi)}{a}+\frac{2\sigma}{a}\ln\left(\frac{2\pi\dot{x}}{\omega_0 a}\right). \tag{14}$$

We now proceed to derive $\Delta U_0(\phi)$ by considering the case of constant velocity motion ($\dot{x}=V$). In this case $\phi=D_0/V$ and the friction force [given in Eq. (6)] is equal to the external force F_{ext} given in Eq. (14). This gives rise to

$$Mg[a_v-b_v\ln(V/V_0)]=\frac{2\Delta U_0(\phi)}{a}+\frac{2\sigma}{a}\ln\left(\frac{2\pi V}{\omega_0 a}\right).$$

By using the average contact age ϕ, we can rewrite the above equation as

$$\Delta U_0(\phi)=\frac{a}{2}Mg\left\{a_v-b_v\ln\frac{D_0}{V_0}-A\ln\frac{2\pi D_0}{\omega_0 a}+(b_v+A)\ln\phi\right\}, \tag{15}$$

where $A=2\sigma/aMg$. Given $\Delta U_0(\phi)$, we can write the friction coefficient (which is equal to the external force divided by the weight Mg under a quasistationary approximation) in terms of ϕ,

$$\mu(\phi,\dot{x})=a_v+b_v\ln\frac{\phi V_0}{D_0}+A\ln\frac{\phi\dot{x}}{D_0}. \tag{16}$$

When the velocity is not a constant, the contact age ϕ is assumed to be the state variable that follows the Dieterich-Ruina aging law

$$\dot{\phi}(t)=1-\frac{\dot{x}\phi}{D_0}. \tag{17}$$

By using this equation, the rate dependence of the dynamic friction and the contact time dependence of the static friction can be taken into account properly. In fact, it is obvious that Eq. (16) (which is written under the quasistationary approximation) is identical to Eq. (1) by choosing $a_v=\mu_0$, $A=A'$, $b_v+A=B'$, $V_0=v_c$, and $D_0=d_c$. Thus Eqs. (16) and (17), which form the basis for the phenomenological description of dry friction given in Ref. [7], are equivalent to the Dieterich-Ruina aging (or slowness) law [8,10–12]. This is a strong indication that the phenomenological theory of dry friction discussed in Ref. [7] is not limited to the explanation of experimental results on the paper-on-paper system; it gives a rather general phenomenological picture that can be used for understanding the dynamics involving dry friction on a range of materials. For example, it may be useful for studying the phenomenology of rock friction, which is important in the study of earthquake dynamics.

For the case where σ is comparable to $F_{ext}a$ (this can be thought of as in the static friction regime), we have to use the original equation, i.e., Eq. (13), which can be rewritten as

$$F_{ext}(\phi,\dot{x})=MgA\sinh^{-1}\left\{\frac{\pi\dot{x}}{\omega_0 a}\exp\left[\frac{\Delta U_0(\phi)}{\sigma}\right]\right\}. \tag{18}$$

The friction coefficient is then given as (with the quasistationary approximation)

$$\mu(\phi,\dot{x})=A\,\mathrm{sgn}(\dot{x})\sinh^{-1}\left\{\frac{1}{2}\exp\left[\frac{\overline{\mu}}{A}\right]\right\}, \tag{19}$$

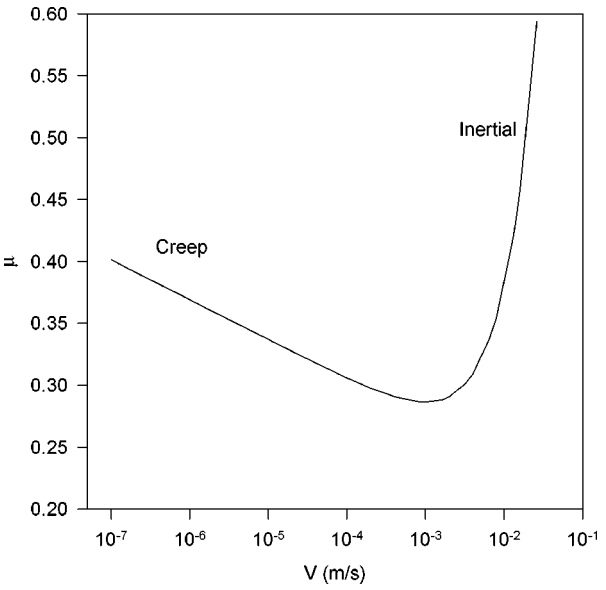

FIG. 2. Friction coefficient μ described by Eq. (23) vs the pulling velocity V when the sliding motion is steady. μ changes from velocity weakening to velocity strengthening at $V=V^*$ ($=1$ mm/s); this gives $\eta=14.0$ s/m.

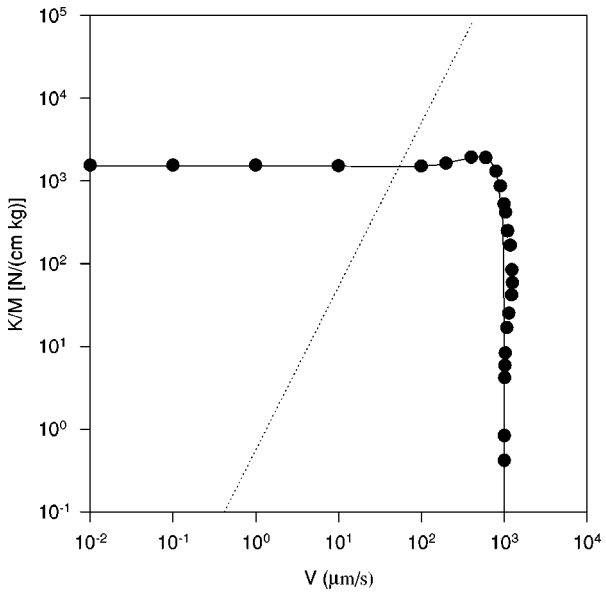

FIG. 3. Dynamical phase diagram in $(V,K/M)$ space, obtained by varying K and V with $M=1.2$ kg. It consists of a creep-dominated regime that can be characterized by the time scale τ_{cr} and an inertial regime with a characteristic time τ_{in} (see the text). The dotted line indicates $\tau_{cr}=\tau_{in}$. The bifurcation curve, which is represented by closed circles, first decreases slightly as V increases in the creep-dominated regime and deflects upward after entering the inertial regime in which it reaches a maximum and drops suddenly. The bifurcation occurs at $K/M\approx 1.53\times 10^3$ N/cm kg when the motion is creep dominated and it happens within 1.01×10^3 μm/s$\leqslant V\leqslant 1.26\times 10^3$ μm/s when inertial motion takes place. The solid line is the theoretical prediction by Rice and Ruina [Eqs. (4) and (5)].

where

$$\bar{\mu}=a_v+b_v\ln\frac{\phi V_0}{D_0}+A\ln\frac{\phi|\dot{x}|}{D_0}. \tag{20}$$

Here $\bar{\mu}$ is an approximation of μ we describe in Eq. (16). In this static friction regime, the velocity $\dot{x}$ is very small and it can also change its sign, thus the equation for ϕ needs to be modified. It is reasonable to simply use

$$\dot{\phi}(t)=1-\frac{|\dot{x}|\phi}{D_0}. \tag{21}$$

Although the regularized friction law stated in Eqs. (19)–(21) has been briefly mentioned by Rice and Ben-Zion [12], it appears as a natural result of the phenomenological theory discussed in Ref. [7].

There are a few advantages of using Eqs. (19)–(21) to describe the friction force: (i) There is no need to make a distinction between static and dynamic frictions, thus there is no *stopping* condition (which is used to indicate the crossover from the dynamic friction regime to the static friction regime) to worry about; (ii) the contact age is a well-defined quantity with Eq. (21); and (iii) there is no numerical singularity in the dynamical equations for the sliding block when the velocity goes to zero and changes sign. To include the inertial regime, we have to take into account the velocity strengthening described by Eq. (7); we include this effect by simply adding a damping term $\eta\dot{x}$ in Eq. (19) (a similar idea has been used in Ref. [17]).

IV. PHASE DIAGRAM OF DRY FRICTION DYNAMICS

We now present the numerical results from the simulation of the block-spring system. Using the friction law described in the preceding section, we can write down the dynamical equations of the block-spring system shown in Fig. 1:

$$M\ddot{x}(t)=K(Vt-x)-\mu(\phi,\dot{x})Mg, \tag{22}$$

where

$$\mu(\phi,\dot{x})=A\,\mathrm{sgn}(\dot{x})\sinh^{-1}\left\{\frac{1}{2}\exp\left[\frac{\bar{\mu}}{A}\right]\right\}+\eta\dot{x}, \tag{23}$$

$$\bar{\mu}=a_v+b_v\ln\frac{\phi V_0}{D_0}+A\ln\frac{\phi|\dot{x}|}{D_0}, \tag{24}$$

and

$$\dot{\phi}(t)=1-\frac{|\dot{x}|\phi}{D_0}. \tag{25}$$

We compare our result for the friction coefficient $\mu=\mu(D_0/V,V)$ with the experimental results when the sliding motion is steady ($\dot{x}=V$ and $\phi=D_0/V$). All the coefficients in the friction law are determined precisely in experiments for the paper-on-paper system except for the value of η, which is determined as follows. We consider the deflection point at $V=V^*$ from velocity weakening to velocity strengthening; this is determined using $d\mu(D_0/V,V)/dV|_{V=V^*}=0$. This leads to

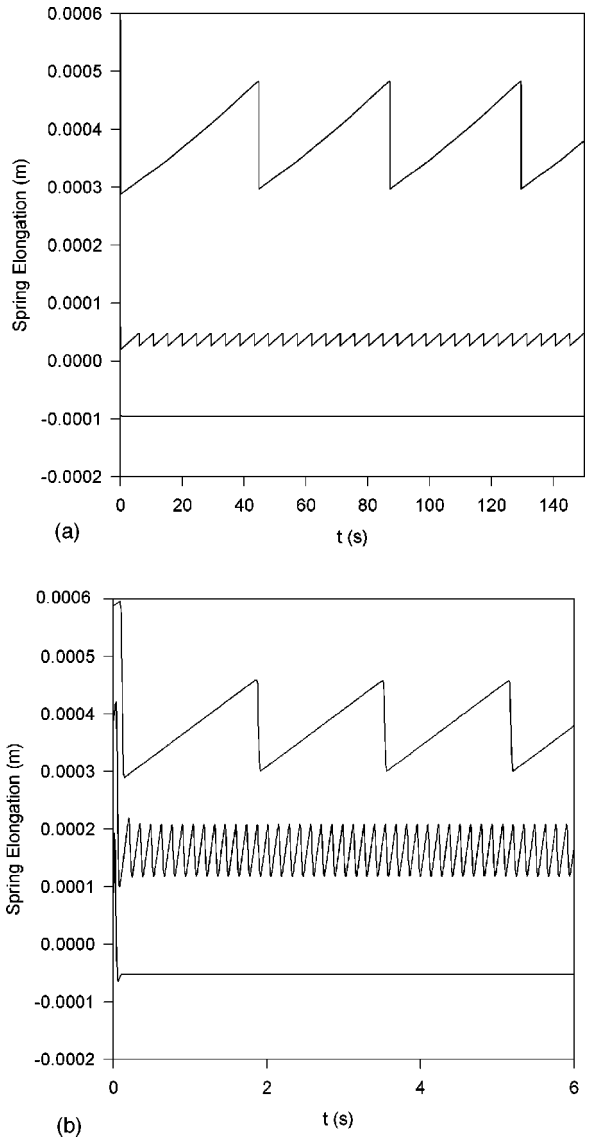

FIG. 4. (a) Time evolution of the spring elongation, when crossing the bifurcation curve in the low-velocity regime. $V=5.0\ \mu$m/s, $M=1.2$ kg, and (from the upper to the lower curve) $K=10^2$, 10^3, and 10^4 N/cm. The lowest curve has been shifted vertically by the amount -1.0×10^{-4} for the sake of clarity. (b) Transition from stick-slip motion to steady sliding in the high-velocity regime. $K=10^2$ N/cm, $M=1.2$ kg, and (from the upper to the lower curve) $V=10^2$, 10^3, and $10^4\ \mu$m/s. The lowest and the second lowest curves have been shifted vertically by the amounts -5.0×10^{-4} and -2.0×10^{-4}, respectively, for the sake of clarity.

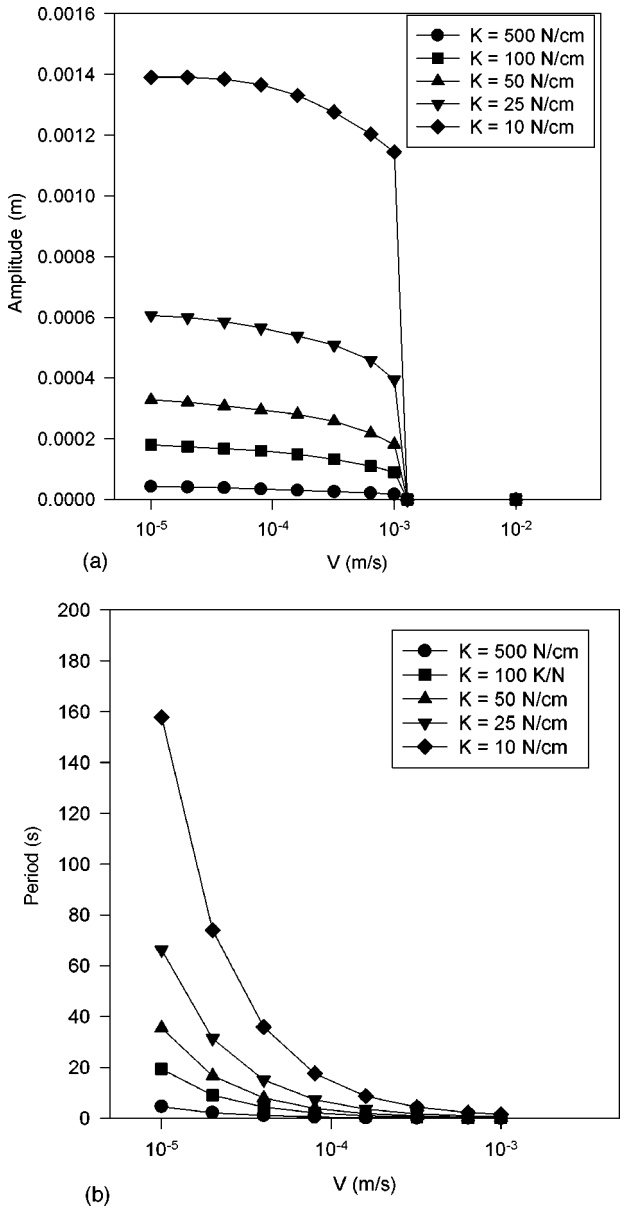

FIG. 5. (a) Amplitude of the stick-slip oscillations vs the pulling velocity V at various values of K. The amplitude approaches zero continuously as K increases, whereas the transition from stick-slip to steady sliding as V is increased is rather sharp. (b) Period of the stick-slip oscillations vs the pulling velocity V at various K. The period approaches zero continuously as either K or V increases.

$$\eta=\frac{b_v}{2V^*}\frac{\exp\left[\frac{\bar{\mu}}{A}\right]}{\sqrt{\frac{1}{4}\exp\left[\frac{2\bar{\mu}}{A}\right]+1}}, \tag{26}$$

where $\bar{\mu}=a_v-b_v\ln(V^*/V_0)$. Substituting the experimental values $a_v=0.369$, $b_v=0.014$, $V_0=1\ \mu$m/s, $V^*=1$ mm/s [7], and $A=0.011$ [15] into Eq. (26) gives $\eta=14.0$ s/m.

Using the values given above, the friction coefficient $\mu(D_0/V,V)$ in the steady sliding region is shown in Fig. 2, which shows excellent agreement with experiments [7]. The logarithmic velocity weakening behavior of $\mu(D_0/V,V)$ can be found at low velocities ($\leqslant$0.1 mm/s); in this regime, the motion of the slider is creep dominated and the effect of the damping term ηV is negligible. In the high-velocity regime, $\mu(D_0/V,V)$ becomes an increasing function of V, which behaves as ηV asymptotically. Hence the experimentally observed dynamic friction coefficient $\mu_d(V)$ [7] can be described by our simple expression of $\mu(D_0/V,V)$ without imposing any extra condition. A similar dependence of the steady-state coefficient on V was also observed in a modified Ruina-Dieterich slip law [17].

We explore the dynamical phase diagram in control parameter space $(V,K/M)$ by systematically varying V (from 10^{-2} to $10^5\ \mu$m/s) and K (from 10^{-1} to 10^5 N/cm) with M

$=1.2$ kg (this is the value used in the experiment). The phase diagram is shown in Fig. 3. Stick-slip motion occurs below a bifurcation curve $(K/M)_c(V)$, and steady sliding is found above (or to the right of) it. The closed circles refer to the first steady sliding motions observed with increasing K or V. The phase diagram consists of a creep-dominated regime that can be characterized by the time scale $\tau_{cr}=D_0/V$ at low velocities and an inertial regime with a characteristic time $\tau_{in}=2\pi(M/K)^{1/2}$ at higher velocities. The dotted line indicates $\tau_{cr}=\tau_{in}$. In the creep-dominated (low-velocity) regime, the bifurcation occurs almost at a constant K/M ($\approx 1.53\times 10^3$ N/cm kg). Figure 4(a) shows the bifurcation from stick-slip to steady sliding as K is increased in this regime. The bifurcation curve first slightly decreases in the creep-dominated regime as V is increased and deflects upward after crossing the dotted line. In the inertial regime, the curve increases until it reaches a maximum and then drop suddenly: The bifurcation mainly occurs within a narrow region of V (1.01×10^3 μm/s$\leqslant V\leqslant 1.26\times 10^3$ μm/s). The bifurcation from stick-slip motion to steady sliding in this regime is shown in Fig. 4(b). The theoretical curve calculated using the Rice-Ruina stability [13] (using Eqs. (4) and (5) with $\mu_{ss}(V)=\mu(D_0/V,V)$ and $[\partial\mu(\text{state},V)/\partial V]_{\text{state}=\text{state}(V)}=[\partial\mu(\phi,V)/\partial V]_{\phi=D_0/V}$) is also plotted in Fig. 3. Our numerical result agrees well with the theoretical prediction, except for some slight deviation at high velocities. Our numerical phase diagram also agrees reasonably well with the experimental phase diagram, except for the slope of the experimental bifurcation curve, which we are not able to reproduce with our model.

To investigate the nature of the bifurcation, we have measured the amplitude and period of the stick-slip oscillations by using different K and V. The results are shown in Fig. 5. The amplitude and period decrease as the stiffness K is increased. The amplitude approaches zero continuously as K becomes larger and larger; this suggests that the bifurcation from stick-slip motion to steady sliding by increasing K is a direct Hopf bifurcation. This agrees with previous theoretical and numerical analyses [7,15]. On the other hand, the transition from stick-slip motion with a finite amplitude to steady sliding (with zero amplitude) with increasing pulling velocity V is rather sharp (the transition velocity is between 1.01×10^3 and 1.26×10^3 μm/s). This supports that the bifurcation encountered by increasing velocity is of the inverted Hopf type, as was suggested previously [9,7,18] based on experimental data (but was not understood theoretically). We have shown numerically that the inverted Hopf bifurcation can be obtained within our friction model.

V. CONCLUSION

We extend the phenomenological description of Baumberger and co-workers and construct a simple model that can be used to simulate the dynamics of dry friction in various regimes. We have shown that by associating the thermally activated creeping motion with a damping term that is significant only when the velocity is large, the behavior of the experimentally observed dynamic friction coefficient μ_d can be predicted easily. Our model also gives rise to satisfactory agreement with the experimental phase diagram. Except for the slope of the bifurcation curve observed in experiments, the essential features of the bifurcation in both creep-dominated and inertial regimes can be reproduced using our simple model. We believe that the model will also be very useful for the numerical study of earthquake models, which are often modeled using block-spring systems.

[1] F. P. Bowden and D. Tabor, *Friction and Lubrication of Solids* (Clarendon, Oxford, 1950).

[2] E. Rabinowicz, *Friction and Wear of Materials* (Wiley, New York, 1965).

[3] W. F. Brace and J. D. Byerlee, Science **15**, 990 (1966).

[4] C. H. Scholz, *The Mechanics of Earthquakes and Faulting* (Cambridge University Press, Cambridge, 1990), Chap. 2 and references therein.

[5] J. T. Oden and J. A. C. Martins, Comput. Methods Appl. Mech. Eng. **52**, 527 (1985).

[6] J. H. Dieterich, Pure Appl. Geophys. **116**, 790 (1978); J. H. Dieterich, J. Geophys. Res. **84**, 2161 (1979); J. H. Dieterich, in *Mechanical Behavior of Crustal Rocks*, edited by N. L. Carter, M. Friedman, J. M. Logan, and D. W. Stearns, Geophysics Monograph No. 24 (AGU, Washington, DC, 1981), p. 103.

[7] F. Heslot, T. Baumberger, B. Perrin, B. Caroli, and C. Caroli, Phys. Rev. E **49**, 4973 (1994).

[8] A. L. Ruina, J. Geophys. Res. **88**, 10 359 (1983).

[9] T. Baumberger, F. Heslot, and B. Perrin, Nature (London) **367**, 544 (1994).

[10] N. M. Beeler, T. E. Tullis, and J. D. Weeks, Geophys. Res. Lett. **21**, 1987 (1994).

[11] G. Perrin, J. R. Rice, and G. Zheng, J. Mech. Phys. Solids **43**, 1461 (1995).

[12] J. R. Rice and Y. Ben-Zion, Proc. Natl. Acad. Sci. USA **93**, 3811 (1996).

[13] J. R. Rice and A. L. Ruina, J. Appl. Mech. **50**, 343 (1983).

[14] J.-C. Gu, J. R. Rice, A. L. Ruina, and S. T. Tse, J. Mech. Phys. Solids **32**, 167 (1984).

[15] T. Baumberger, C. Caroli, B. Perrin, and O. Ronsin, Phys. Rev. E **51**, 4005 (1995).

[16] T. Baumberger and L. Gautier, J. Phys. I **6**, 1021 (1996).

[17] F. G. Horowitz and A. L. Ruina, J. Geophys. Res. **94**, 10 279 (1989).

[18] T. Baumberger, in *Physics of Sliding Friction*, edited by B. N. J. Persson and E. Tosatti (Kluwer, Dordrecht, 1996).